(12)

DTNSRDC-84/048

AD-A143 974

# DAVID W. TAYLOR NAVAL SHIP RESEARCH AND DEVELOPMENT CENTER

Bethesda, Maryland 20084

## NUMERICAL AND EXPERIMENTAL SIMULATION OF CIRCULATION CONTROL ROTOR PNEUMODYNAMICS

by

C.B. Watkins and S.K. Dutta
Howard University
K.R. Reader

APPROVED FOR PUBLIC RELEASE: DISTRIBUTION UNLIMITED

Reprint from Paper AIAA-83-2551 Presented at
AIAA Aircraft Design, Systems and
Technology Meeting, Fort Worth,
Texas, 17-19 October 1983





AVIATION AND SURFACE EFFECTS DEPARTMENT
RESEARCH AND DEVELOPMENT REPORT

July 1984

DTNSRDC-84/048

NUMERICAL AND EXPERIMENTAL SIMULATION OF CIRCULATION CONTROL ROTOR PNEUMODYNAMICS

## MAJOR DTNSRDC ORGANIZATIONAL COMPONENTS

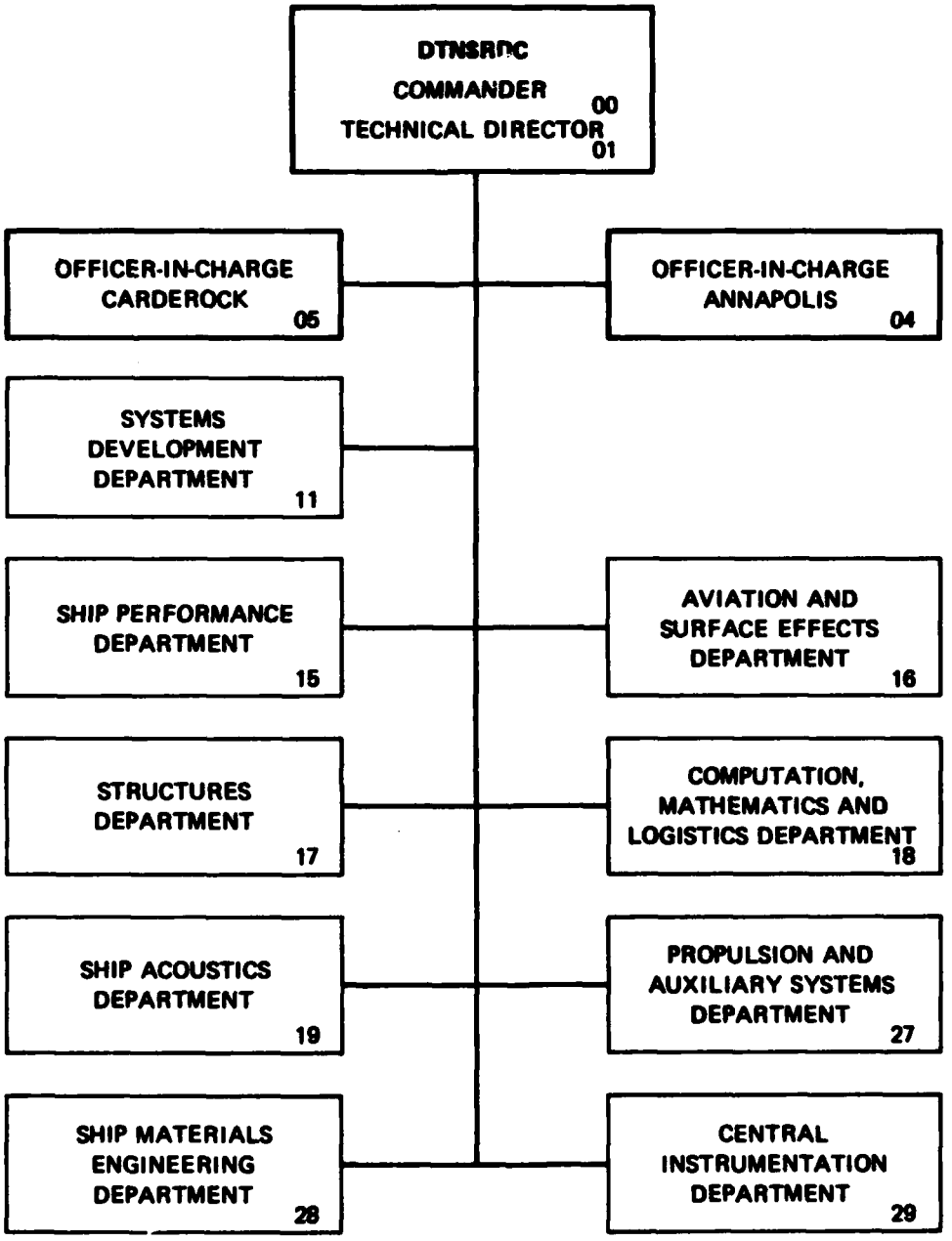


GPO 867-440

NDW-DTNSRDC 3900/43b (Rev. 2-80)

UNCLASSIFIED

SECURITY CLASSIFICATION OF THIS PAGE (When Data Entered)

| REPORT DOCUMENTATION PAGE | | READ INSTRUCTIONS BEFORE COMPLETING FORM |
|---|---|---|
| 1. REPORT NUMBER<br>DTNSRDC-84/048 | 2. GOVT ACCESSION NO.<br>AD-A143 974 | 3. RECIPIENT'S CATALOG NUMBER |
| 4. TITLE (and Subtitle)<br>NUMERICAL AND EXPERIMENTAL SIMULATION OF CIRCULATION CONTROL ROTOR PNEUMODYNAMICS | | 5. TYPE OF REPORT & PERIOD COVERED<br>Oct 1983 - Oct 1984<br>6. PERFORMING ORG. REPORT NUMBER<br>Aero Report-1293 |
| 7. AUTHOR(s)<br>C.B. Watkins and S.K. Dutta<br>Howard University<br>K.R. Reader | | 8. CONTRACT OR GRANT NUMBER(s)<br>N00167-82-M-5006 |
| 9. PERFORMING ORGANIZATION NAME AND ADDRESS<br>David W. Taylor Naval Ship<br>Research and Development Center<br>Bethesda, Maryland 20084 | | 10. PROGRAM ELEMENT, PROJECT, TASK AREA & WORK UNIT NUMBERS<br>ARPA Order No. 4238<br>Program Element 62711E<br>Work Unit 1605-101 |
| 11. CONTROLLING OFFICE NAME AND ADDRESS | | 12. REPORT DATE<br>July 1984<br>13. NUMBER OF PAGES<br>15 |
| 14. MONITORING AGENCY NAME & ADDRESS(if different from Controlling Office) | | 15. SECURITY CLASS. (of this report)<br>UNCLASSIFIED<br>15a. DECLASSIFICATION/DOWNGRADING SCHEDULE |

16. DISTRIBUTION STATEMENT (of this Report)

APPROVED FOR PUBLIC RELEASE: DISTRIBUTION UNLIMITED

17. DISTRIBUTION STATEMENT (of the abstract entered in Block 20, if different from Report)

18. SUPPLEMENTARY NOTES

Reprint from Paper AIAA-83-2551 Presented at AIAA Aircraft Design, Systems and Technology Meeting, Fort Worth, Texas, 17-19 October 1983.

19. KEY WORDS (Continue on reverse side if necessary and identify by block number)

Circulation Control Rotor
Cam-Type Valving System
Higher Harmonic Control
Pneumatics

20. ABSTRACT (Continue on reverse side if necessary and identify by block number)

Numerical solution of the quasi-one-dimensional unsteady compressible flow equations applied to flow through the control valve and slotted air supply duct of a circulation control rotor is described. An implicit finite-difference method is used for the numerical solution. Solutions are compared with basic experimental results obtained for a mock-up of a circulation control rotor and its pneumatic valving system. Details of the experiment are presented and the experimental and numerical results are discussed.

DD FORM 1 JAN 73 1473 EDITION OF 1 NOV 65 IS OBSOLETE
S/N 0102-LF-014-6601

UNCLASSIFIED

SECURITY CLASSIFICATION OF THIS PAGE (When Data Entered)

TABLE OF CONTENTS



LIST OF FIGURES

# NUMERICAL AND EXPERIMENTAL SIMULATION OF CIRCULATION CONTROL ROTOR PNEUMODYNAMICS

C.B. Watkins*
Howard University, Washington, D.C.

K.R. Reader**
David W. Taylor Naval Ship Research and Development Center
Bethesda, Md.

S.K. Dutta†
Howard University, Washington, D.C.

## Abstract

Numerical solution of the quasi-one-dimensional unsteady compressible flow equations applied to flow through the control valve and slotted air supply duct of a circulation control rotor is described. An implicit finite-difference method is used for the numerical solution. Solutions are compared with basic experimental results obtained for a mock-up of a circulation control rotor and its pneumatic valving system. Details of the experiment are presented and the experimental and numerical results are discussed.

## NOMENCLATURE

| | |
|---|---|
| $A$ | Cross-sectional area of duct |
| $A_e$ | Effective expansion area at valve exit |
| $A_v$ | Valve area |
| $a$ | Jacobian matrix $\partial F/\partial U$ |
| $b$ | Jacobian matrix $\partial G/\partial U$ |
| $c_f$ | Duct friction factor |
| $C_s$ | Slot discharge coefficient |
| $C_{s_{tip}}$ | Tip discharge coefficient |
| $c_v$ | Specific heat at constant volume |
| $D_H$ | Hydraulic diameter of duct |
| $e$ | Internal energy per unit volume |
| $F$ | Flux times area vector |
| $G$ | Vector of nonhomogeneous terms in flow equations |
| $h$ | Heat transfer coefficient |
| $H_D$ | Average duct height |
| $h_{0_{p\ell}}$ | Total enthalpy in pressure supply plenum minus rotational kinetic energy at duct entrance |
| $k$ | Thermal conductivity |
| $m$ | Mass flow rate per unit area in duct |
| $m_I$ | Mass flow rate per unit area computed from isentropic flow theory |
| $m_s$ | Mass flow rate per unit area through slot |
| $m_v$ | Mass flow rate per unit area through valve |
| $p$ | Static pressure in central duct |
| $p_{crit}$ | Critical pressure at valve exit |
| $p_{ext}$ | External pressure at slot exit |
| $p_0$ | Total pressure in duct |
| $T$ | Duct static temperature |
| $T_0$ | Duct total temperature |
| $t$ | Time |
| $U$ | Vector of dependent variables |
| $V$ | Vector of diffusion terms |
| $v_x$ | Average duct velocity in spanwise or x direction |
| $v_y$ | Approximate average duct velocity in chordwise or y direction |
| $w_s$ | Slot width |
| $x$ | Spanwise coordinate |
| $x_e$ | Coordinate at duct entrance |
| $x_t$ | Coordinate at duct tip |
| $y$ | Chordwise coordinate |
| $\gamma$ | Ratio of specific heats |
| $\rho$ | Density |
| $\omega$ | Angular frequency |

Subscripts

| | |
|---|---|
| $I$ | Variable from isentropic flow at valve exit |
| $p\ell$ | Variable in pressure supply plenum or rotor hub |

## Introduction

Circulation control aerodynamics applied to rotary-wing aircraft offers the advantages of a simple and effective solution to such problems as high vibration levels, retreating blade stall, hub/pylon drag and incorporating higher harmonic control. When the technology is applied to stopped-rotor, VTOL aircraft such as the X-wing, the historical stopped-rotor limitations of aeroelastic divergence, flutter, blade dynamic instability, and critical resonance conditions during rpm reduction are alleviated. Reader, et al[1] trace the development of circulation control rotor technology from its inception[2] through its application in the recent past to programs at the David W. Taylor Naval Ship Research and Development Center (DTNSRDC). Current studies at DTNSRDC involve application of circulation control to rotary-wing aircraft for a variety of missions.

The concept of circulation control (CC) as applied to helicopters and rotary-wing aircraft which convert to fixed-wing aircraft by stopping the rotor are essentially the same. Both types of aircraft utilize a shaft-driven rotor with blades having CC airfoils which generate lift through the Coanda effect. The CC airfoils employ a rounded trailing edge with a thin jet of air tangetially ejected from a spanwise slot adjacent to the rounded (Coanda) surface. The jet of air suppresses boundary layer separation and moves the rear stagnation streamline toward the lower surface, thereby increasing lift. Lift is increased in proportion to the mass flow rate of compressed air in the jet. Pitch and roll control requirements are obtained

*Professor of Mechanical Engineering, Member AIAA
**Aerospace Engineer, Member AHS
†Graduate Assistant, Student Member AIAA

by cyclic modulation of the mass flow rate with valves. Higher harmonic cyclic control can be similarly applied for reducing blade stresses, transmitted shears, vibration and power requirements.

In view of the importance of the system for pneumatic control and distribution of Coanda blowing air in a CC airfoil, suprisingly little attention has been given in the open literature to the physics of these systems. Therefore, to create a knowledge base sufficient for preliminary design requires basic experimentation aimed at understanding the phenomenology involved in the control and distribution of airflow in CC rotors, i.e., the "pneumodynamics" of CC rotors. The results of these experiments can also serve as baseline data against which theoretical models developed for design analysis can be evaluated. Reader[3] conducted such experiments, in which mass flow and pressure measurements were obtained for a simple mock-up of a rotor-blade and its pneumatic control valves.

Theoretical models for computer simulation of the pneumodynamics of CC airflow control systems and rotors have been developed by a few DTNSRDC contractors. Perhaps the most noteworthy among these are two computer codes which include modeling of the complex, unsteady, distributed fluid dynamic phenomena in the rotor blade ducting system, the SUPERFLOWS code developed by the Lockheed California Company[4] and the more recent High Frequency Pneumodynamic Analysis (HFPA) code described herein. The HFPA code represents an attempt to improve on the physical and numerical modeling used in the earlier SUPERFLOWS code, by eliminating modeling inconsistencies and by adopting an efficient contemporary computational fluid dynamics formulation suitable for applications involving high frequency cyclic control.

The present paper gives some details of the physical and numerical model used in the HFPA code and compares computed results obtained by applying the code to Reader's[3] experimental configuration with the experimental data. A description of the experiment is included.

## Theory

### Basic Equations

The HFPA code solves the quasi-one-dimensional, compressible fluid dynamic equations in conservation law form, for unsteady flow in a spanwise blowing air supply duct, internal to a rotor blade with a Coanda slot. These equations have the representation

$$U_{,t} + \frac{1}{A} F_{,x} + G + V = 0 \qquad (1)$$

where the vector of dependent variables is

$$U = \begin{bmatrix} \rho \\ m \\ e \end{bmatrix}$$

and the flux times area vector is given by

$$F = \begin{bmatrix} mA \\ \left(\frac{m^2}{\rho} + p\right) A \\ (e + p) \frac{m}{\rho} A \end{bmatrix}$$

The vector of nonhomogeneous terms, which includes the effects of blade rotation at angular velocity $\omega$, wall skin friction factor $c_f(x)$, wall heat transfer coefficient $h(x)$, and mass flux through the slot $m_s(x,t)$ is

$$G = \begin{bmatrix} \frac{m_s w_s}{A} \\ -\frac{p}{A}\frac{dA}{dx} + \frac{m_s w_s m}{\rho A} + \frac{2c_f m^2}{D_H \rho} - \rho\omega^2 x \\ \frac{m_s w_s (e+p)}{A\rho} - m\omega^2 x + \frac{4h}{D_H}(T - T_w) \end{bmatrix}$$

For completeness the vector of axial diffusion terms is included, although it is insignificant in the present problem. It is

$$V = \begin{bmatrix} 0 \\ \frac{4}{3}\left(\frac{m}{\rho}\right)_{,xx} \\ -\frac{4}{3}\left(\frac{m}{\rho}\left(\frac{m}{\rho}\right)_{,x}\right)_{,x} - kT_{,xx} \end{bmatrix}$$

The equation of state is

$$p = (\gamma - 1)\left(e - \frac{m^2}{2\rho} - \rho\frac{v_y^2}{2}\right) \qquad (2)$$

In the above relations the conservative variables m and e are defined as

$$m = \rho v_x$$

$$e = \rho\left(c_v T + \frac{v_x^2}{2} + \frac{v_y^2}{2}\right)$$

and $w_s(x,t)$ and $m_s(x,t)$ are the local (with respect to spanwise x location) slot width and blowing mass flux, respectively

The small average chordwise velocity component inside the duct can be crudely approximated as

$$v_y \simeq \frac{w_s m_s}{2\rho H_D} \qquad (3)$$

in which $H_D(x)$ is the local effective height of the duct.

The mass flux distribution through the Coanda slot is assumed to be sufficiently well represented by one-dimensional isentropic flow theory with a discharge coefficient $C_s(x)$.

$$m_s(x,t) = C_s m_I(p_0, T_0, p_{ext}) \qquad (4)$$

The above functional relationship is the usual expression for isentropic flow expanding through a nozzle from a plenum (in this case the duct interior) to ambient conditions (in this case the exterior of the rotor blade). $p_0$ and $T_0$ are the local total pressure and temperature respectively and $p_{ext}(x,t)$ is the external pressure at the exit of the Coanda slot. For choked slot conditions the dependence of Eq. (4) on $p_{ext}$ is eliminated.

The blowing slot for a circulation control rotor is generally designed to be flexible, i.e., its width at a particular spanwise location can depend on internal duct pressure at the slot entrance, external pressure at the slot exit and the local pressure distribution over the rear surface of the airfoil. This type of slot can easily be accommodated within the framework of the present model; the HFPA code, although used herein to obtain simple constant slot height results, contains provisions for calculations involving the more general case of a flexible slot.

The computer code will also handle the more general case wherein minor flow losses occur between the air supply duct and the slot; for example, due to partial obstructions caused by structural members interposed between the air supply duct and the slot entrance.

Boundary Conditions

At the upstream boundary $x = x_e$, a plenum supplies Coanda blowing air to the duct through a valving system. The valve opening area has constant and rotor-azimuth-dependent components regulated by the collective and cyclic components respectively of the aircraft control system. The mass flow and duct pressures are thus determined by these valve settings. Figure 1 shows the three different types of idealized valve models considered in the present analysis, where $A_v(t)$ is the controlled value of the valve opening and $A_e$ is the fixed effective opening at the duct entrance. Like the slot flow, one-dimensional isentropic flow theory with a discharge coefficient is used to represent flow through the valve. The valve mass flux is

$$m_v = C_v m_I(p_{0_{p\ell}}, T_{0_{p\ell}}, p(x_e,t)) \qquad (5)$$

where $p_{0_{p\ell}}$ and $T_{0_{p\ell}}$ are the total pressure and temperature in the air supply plenum in the rotor hub. For choked flow through the valve there is no dependence on the back pressure in the duct entrance downstream of the valve, $p(x_e,t)$. The critical pressure in the duct at the valve for choked flow is

$$p_{crit} = p_{0_{p\ell}} \left(\frac{2}{\gamma+1}\right)^{\gamma/\gamma-1} \qquad (6)$$

An expansion wave will occur at the valve exit for choked flow. The pressure $p_v$ just upstream of the valve exit is

$$p_v = p(x_{e,t}) \text{ for } p(x_e,t) > p_{crit} \qquad (7)$$

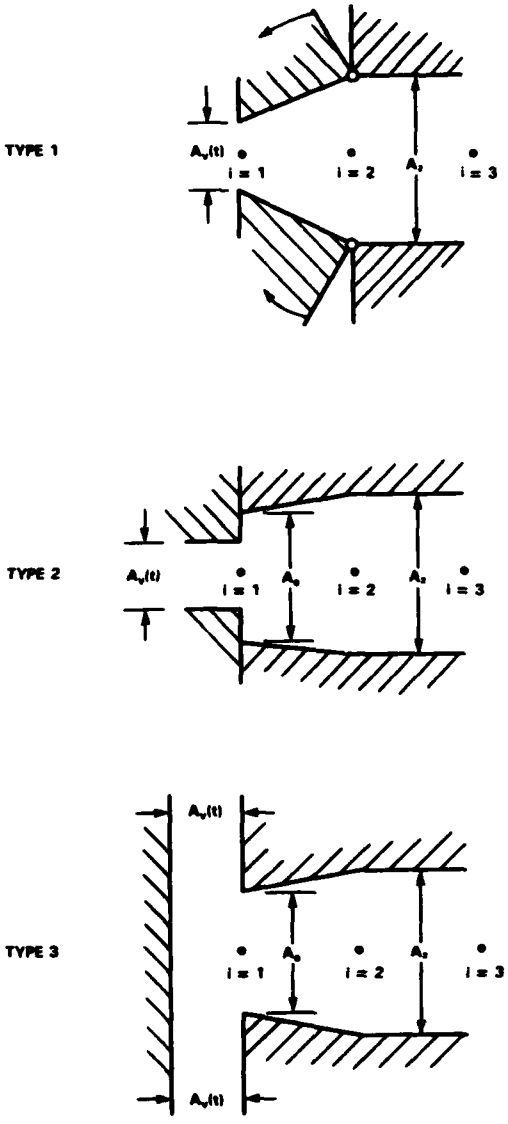


Fig. 1 Valve Flow Models

$$p_v = p_{crit} \text{ for } p(x_e,t) < p_{crit} \qquad (8)$$

The remaining dependent variables at the same location can be calculated from

$$\rho_v = p_v^{1/\gamma} \left(\rho_{0_{p\ell}} p_{0_{p\ell}}^{-1/\gamma}\right) \qquad (9)$$

$$e_v = \rho_v h_{0_{p\ell}} - p_v \qquad (10)$$

The flux vector, F, in Eq. (1) must be given special attention at the duct entrance to ensure a consistent

transition from the valve to the duct. For valve types 1 and 2 in Fig. 3

$$F(x_e,t) = m_v A_v \begin{bmatrix} 1 \\ m_v/C_v \\ \rho_v \\ \dfrac{e_v+p_v}{\rho_v} \end{bmatrix} + \begin{bmatrix} 0 \\ p(x_e,t)A_e \\ \\ 0 \end{bmatrix} \quad (11)$$

For valve type 3 in Fig. 1, Eq. (11) must be modified so that the second entry in the first column vector on the right hand side is zero.

The downstream boundary condition at $x = x_t$, the rotor tip, must take into account a possible blowing slot with area $A_{s_{tip}}$ incorporated into the tip cap. Therefore, at the tip

$$m_{tip} = C_{s_{tip}} m_I(p_0(x_t,t), T_0(x_t,t), p_{ext}(x_t,t)) \quad (12)$$

$$F(x_t,t) = m_{tip} A_{s_{tip}} \begin{bmatrix} 1 \\ \dfrac{m(x_t,t)}{\rho(x_t,t)} \\ \\ \dfrac{e(x_t,t) + p(x_t,t)}{\rho(x_t,t)} \end{bmatrix} + \begin{bmatrix} 0 \\ p(x_t,t)A(x_t) \\ \\ 0 \end{bmatrix} \quad (13)$$

where $A_{s_{tip}} = 0$ if there is no tip slot.

## Numerical Analysis

### Finite-Difference Method

In applying the theory of the previous section to the analysis of a rotor blade, the entire blade, including the transition duct (ducting from hub plenum to airfoil portion of rotor blade) is discretized by dividing it into spanwise (radial) segments. The governing differential equations are solved by finite differences at the grid points located at segment boundaries, including the valve exit and the blade tip.

Implicit finite-difference methods, in principle, offer the advantage of no restriction on integration time step. Since in the present problem time-dependent solutions of the governing equations are of interest for dynamic problems of system response to high frequency control inputs, and it is not desirable to link integration time step to the spatial grid, an implicit method was chosen. Candidate methods include those developed by Briley and McDonald,[5] Beam and Warming,[6] and more recently by McCormack.[7,8] In the present research, the method of Beam and Warming[6] was selected and applied to the governing equations in the form given by Eq. (1). In applying this method, the rotor duct is discretized such that it is divided into J elements with J+1 grid points, including a grid point at the entrance to the duct and one at the tip. Following Beam and Warming,[6] the solution is advanced from time level n to time level n+1 implementing the "delta" form of the difference equations where at each grid point i

$$U_i^{n+1} = U_i^n + \Delta U_i^n \quad (14)$$

for

$$i = 1,2, \ldots, i_{max} = J+1$$

and

$$\Delta U_i^n = \frac{\theta\Delta t}{1+\xi}\left[\frac{1}{A_i}\frac{\partial}{\partial x}(-\Delta F_i^n) - \Delta G_i^n\right] + \frac{\Delta t}{1+\xi}\left[\frac{1}{A_i}\frac{\partial}{\partial x}(-F_i^n) - G_i^n\right] + \frac{\xi}{1+\xi}\Delta U_i^{n-1} - \Delta t\, V_i^n \quad (15)$$

The contribution of diffusion terms is assumed minor in importance and, therefore, sufficiently well approximated by an explicit evaluation with no serious impact on stability. In Eq. (15), the implicit Beam and Warming three-level, second-order-accurate scheme is obtained by specifying $\theta$=1, $\xi$=1/2. A fully implicit one-level scheme suitable for starting the calculating or changing integration time step is obtained by specifying $\theta$=1, $\xi$=0. Defining the Jacobians

$$a_i = \left.\frac{\partial F}{\partial U}\right|_i \text{ and } b_i = \left.\frac{\partial G}{\partial U}\right|_i$$

and employing modified central differencing on a variable grid where, for example,

$$\left.\frac{\partial F}{\partial x}\right|_i = \frac{F_{i+1}-F_{i-1}}{x_{i+1}-x_{i-1}}$$

then Eq. (15) leads to the following system of difference equations which will, when modified using the boundary conditions, have block-tridiagonal form.

$$L_{i-1}\Delta U_{i-1} + M_i \Delta U_i + N_{i+1}\Delta U_{i+1} = H_i, \quad i=2,\ldots i_{max}-1 \quad (16)$$

where L, M, and N are the 3x3 matrices,

$$L_{i-1} = -\frac{\theta\Delta t}{1+\xi}\frac{1}{A_i}\frac{a_{i-1}^n}{x_{i+1}-x_{i-1}}$$

$$M_i = \frac{\theta\Delta t}{1+\xi}(b_i^n + I)$$

$$N_{i+1} = \frac{\theta\Delta t}{1+\zeta}\ \frac{1}{A_i}\ \frac{a^n_{i+1}}{x_{i+1}-x_{i-1}}$$

and the column vector $H_i$ is

$$H_i = \frac{\Delta t}{1+\zeta}\left[\frac{1}{A_i}\left(\frac{F^n_{i-1}-F^n_{i+1}}{x_{i+1}-x_{i-1}}\right) - G^n_i\right] + \frac{\zeta}{1+\zeta}\ \Delta U^{n-1}_i - \Delta t\ V^n_i + D_i$$

where numerical damping as recommended by Beam and Warming[6] has been added in the form

$$D_i = (x_{i+1}-x_{i-1})^4\ \frac{\Omega}{128}\frac{\partial^4 U_i}{\partial x^4}$$

In the present work, after some experimentation, the damping coefficient $\Omega$ was set equal to zero.

Numerical Boundary Conditions

At the upstream boundary, the boundary conditions specified as Eqs. (5), (9), and (10) are insufficient for the numerical solution. Three conditions are needed whereas only two of these equations are independent. A common and physically consistent procedure for obtaining the extra condition needed for flow at a subsonic inlet is to use one-sided differences as applied by White and Anderson[8] or to use the method of characteristics. However, in the present calculation the presence of the valve at the inlet apparently renders these procedures useless since they could not be made to work.

Another approach, which proved to be more fruitful, is to derive an approximate auxiliary relationship based on ignoring the time-dependent term in the momentum equation between the first two grid points. The consequence of this is to produce an error in the calculation of transients between the first two grid points. The global effect of this approximation can be minimized by maintaining a relatively fine grid spacing between these points, where possible. In deriving this approximation, the steady flow momentum equations corresponding to the three valve types in Fig. 1 are written between the grid point i=1 at the entrance and the next grid point i=2 immediately downstream. The resulting expressions are:

Type 1 valve

$$\frac{m_I^2}{\rho_I} C_v A_v + p_1 A_v + \frac{(p_1+p_2)}{2}(A_2-A_v) = \frac{m_2^2}{\rho_2} A_2 + p_2 A_2 + \frac{(A_1+A_2)}{2}\ \frac{\rho_2\omega^2}{2}\ (x_1^2-x_2^2) - 2\,\frac{C_f m_2^2}{\rho_2 D_H}\ (x_1-x_2) \qquad (17)$$

Type 2 valve

$$\frac{m_I^2}{\rho_I} C_v A_v + p_1 A_e + \frac{(p_1+p_2)}{2}(A_2-A_e) = \frac{m_2^2}{\rho_2} + p_2 A_2 + \frac{(A_1+A_2)}{2}\ \frac{\rho_2\omega^2}{2}\ (x_1^2-x_2^2) - 2\cdot\frac{C_f m_2^2}{\rho_2 D_H}(x_1-x_2) \qquad (18)$$

Type 3 valve

$$p_1 A_e + \frac{(p_1+p_2)}{2}(A_2-A_e) = \frac{m_2^2}{\rho_2} A_2 + p_2 A_2 + \frac{(A_e-A_2)}{2}\ \frac{\rho_2\omega^2}{2}\ (x_1^2-x_2^2) - 2\ \frac{c_f m_2^2}{\rho_2 D_H}\ (x_1-x_2) \qquad (19)$$

In the above expressions, in general, $x_1 = x_e$, and

$$p_1 = p(x_e,t) \le p_v$$

where the inequality holds for choked flow.

To apply the upstream boundary conditions, the differential form of Eq. (16), (17) or (18) is combined with Eq. (2) and with the differential forms of Eqs. (5) and (10). This procedure transforms the boundary conditions into delta form and enables the dependent variables at i=1, $\Delta U_1$ to be eliminated from the delta difference equation for i=2.

$$F_{i_{max}} = m_{tip} A_{s_{tip}} \begin{bmatrix} 1 \\ \dfrac{m_{i_{max}-1}}{\rho_{i_{max}-1}} \\ \dfrac{e_{i_{max}-1} + p_{i_{max}-1}}{\rho_{i_{max}-1}} \end{bmatrix} + \begin{bmatrix} 0 \\ p_{i_{max}} A_{i_{max}} \\ 0 \end{bmatrix} \qquad (20)$$

where $m_{tip}$ is evaluated from the total quantities at $i=i_{max}-1$, and $p_{i_{max}}$ is calculated from an approximate difference form of the momentum equation written between $i_{max}-1$ and $i_{max}$. The Jacobian term at $i_{max}$, $a_{i_{max}}\Delta U_{i_{max}}$ is taken equal to its value at $i_{max}-1$ with a correction for the difference in mass flow between the two points. The net effect of these approximations is to eliminate the dependent variables at $i=i_{max}$, $\Delta U_{i_{max}}$ from the delta difference equation for $i=i_{max}-1$.

By the manipulations just described, the delta difference equation formulations for the new boundary points i=2 and $i=i_{max}-1$ contain first-order accurate approximations for the physical boundary conditions. When these two equations are combined with Eq. (15) for the interior grid points, they constitute an block tridiagonal set of difference equations. A relatively efficient and simple direct solution algorithm can be used to solve such a system of equations.

## Initial Conditions and Convergence

The basic approach followed in obtaining solutions to control inputs consisting of constant collective settings or constant collective settings with superimposed constant amplitude cyclic inputs is to obtain the steady state or time periodic solutions by allowing them to evolve from a transient.

The code starts with the blade essentially at pressure supply conditions. The initial valve position is assumed to be fully open as specified by its Fourier components supplied as input. The solution is then advanced with time as the flow in the blade adjusts itself to reach steady state flow conditions for the fully open valve. If cyclic components are to be considered, the cyclic is imposed after full-open steady state is achieved. The solution is thereafter advanced further with time until periodic conditions are attained. Experience indicates that two cycles of the fundamental frequency are usually sufficient to achieve the desired periodicity; hence, the final solution is taken to be the results during the third cycle. A harmonic analysis of pressures, temperatures, and mass flow rates is performed on the results from this third cycle.

## Experiment

The analytical formulation and the numerical methods described in the previous sections, which are employed in the HFPA code, were validated by applying the code to a basic configuration for which easily-interpretable experimental results were available.[3] In this experiment an investigation was performed using a mock-up of a rotor blade pneumodynamic system incorporating a valve similar to the type 3 valve of Fig. 1. The model consisted of a supply plenum and two rotating cams mounted on the same shaft (allowing a mix of one or two-per-rev profiles to be selected) modulating flow from the plenum through a single nozzle into a stationary plugged pipe having an adjustable slot. The pipe incorporated three total and two static pressure taps distributed along the length of the pipe. The general arrangement and principal dimensions of the model are shown in Fig. 2.

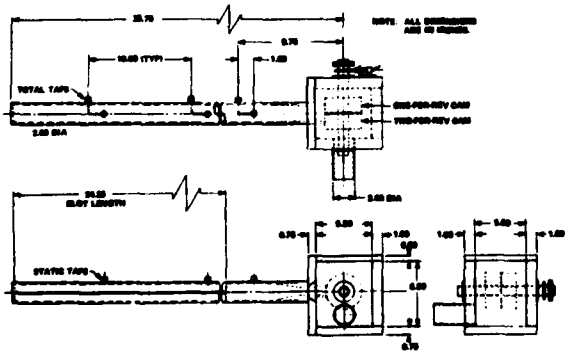

Fig. 2 Experimental Configuration

Dynamic measurements of pipe pressure were obtained by positioning one of the two cams (or portions of both) over the nozzle inlet, setting a plenum pressure and obtaining data for a range of cam rotational speeds. In addition, quasi-dynamic results were obtained by turning the cam in discrete 30-deg increments, each time recording data for this non-rotating condition. Average mass flow data were collected from a venturi located upstream of the plenum.

Fig. 3 shows the effective valve area formed by the one- and two-per-rev cams spaced at a distance of 0.01 in. from the nozzle inlet. The points shown were calculated from the measured cam profile; the area variations are intended to approximate sinusoids as shown.

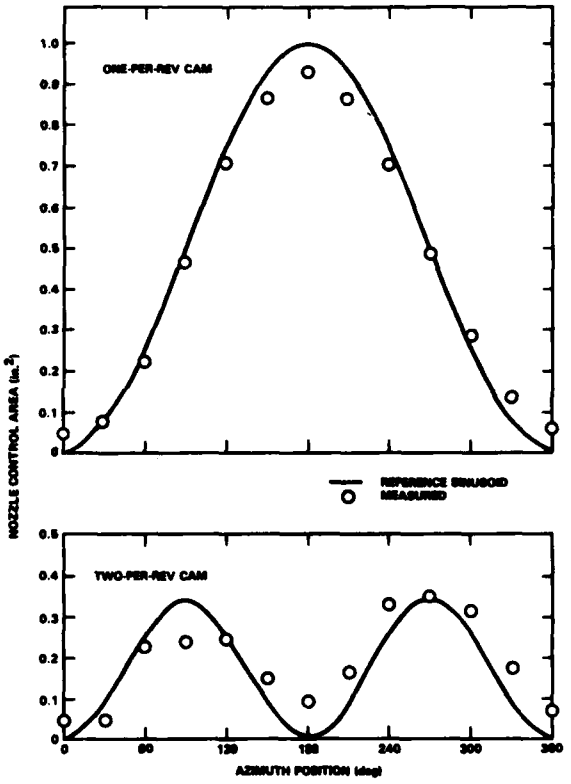


Fig. 3 Nozzle Control Area Variation

## Results and Discussion

Numerical results from the HFPA code were obtained for the experimental configuration of Fig. 2 by discretizing the pipe into 16 segments of approximately equal length ($i_{max}$=17) and using the formulation for valve type 2 of Fig. 1. The pipe was assumed adiabatic and the friction coefficient was represented by the formulas for fully developed flow. The integration timestep for the quasi-dynamic calculation and the initial integration timestep for the dynamic calculations were $5 \times 10^{-4}$ seconds. For the dynamic calculations, valve cycling was imposed

after an elapsed time of 0.025 seconds and the timestep was reduced to 1200 steps per revolution thereafter. Execution consumed approximately two and one-half minutes IBM 3033S CPU time. In spite of the implicit finite-difference scheme, larger timesteps led to numerical instability. Preliminary calculations made to compare HFPA and SUPER-FLOWS results for the sample case of Ref. 4 indicate that, although the present implicit method is still restricted to small timesteps, these timesteps are several times larger than those permitted by the multistep explicit method used in SUPER-FLOWS.

Typical quasi-dynamic numerical and experimental results indicating the dependency of mass flow rates on nozzle control area at a constant slot height of 0.042 in. are displayed for the one-per-rev cam in Fig. 4 and the two-per-rev cam in Fig. 5. The mass flow rates are plotted against the discrete azimuthal cam settings at which the readings and calculations were made. As indicated on the figures the plenum pressures were set to different values for the two cams. The figures indicate the ability of the cam control valve to modulate mass flow so as to track the cyclic variation in valve setting.

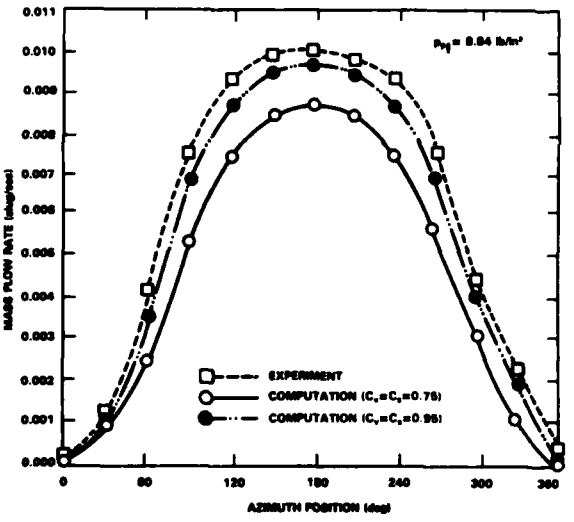


Fig. 4 Quasi-Dynamic Mass Flow Rate vs Cam Position for One-Per-Rev Cam

Figs. 4 and 5 also show the effect of assumed constant values of 0.95 and 0.75 for equal slot and valve discharge coefficients in the HFPA code. The results obtained for the higher values $C_v = C_s = 0.95$ agree more favorably with the experimental results, despite the fact that the lower discharge coefficient is likely more physically realistic. Strict interpretation of $C_s$ and $C_v$ as discharge coefficients is probably not desirable since the various deficiencies and approximations in the computer model can, to some degree, be absorbed by adjusting them. Moreover, the concept of a constant nozzle discharge coefficient is at best only a crude approximation for the actual flow losses which occur over a range of mass flow rates in a dynamic or quasi-dynamic analysis.

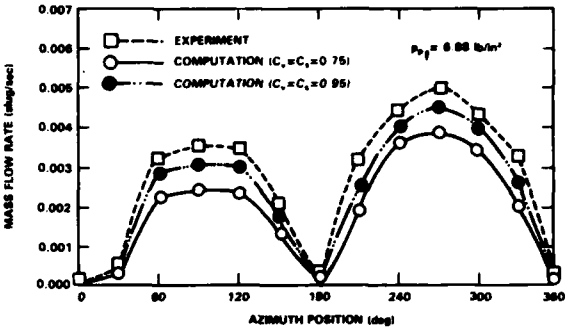


Fig. 5 Quasi-Dynamic Mass Flow Rate vs Cam Position for Two-Per-Rev Cam

Figs. 6 and 7 show the quasi-dynamic results for total pressure corresponding to the mass flow rates of Figs. 5 and 6 again plotted against the discrete azimuthal cam setting at which the readings and calculations were made. These plots also show the better agreement obtained for $C_s = 0.95$ and the ability of the cam arrangement to modulate total pressure so as to track the cyclic variation in valve setting. The total pressures shown in the figure are for the furthest outboard pressure tap location; the measured and computed variation in total pressure along the length of the pipe was minimal.

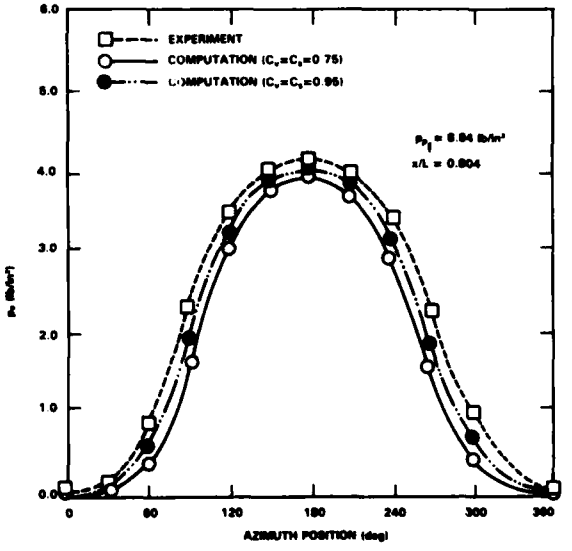


Fig. 6 Quasi-Dynamic Total Pressure vs Cam Position for One-Per-Rev Cam

Fig. 8 is the dynamic counterpart of the quasi-steady total pressures plotted in Fig. 6

and is typical of the dynamic results obtained. Extensive results of the dynamic calculations and measurements will be reported in a subsequent paper; space limitations will not permit their presentation here. The numerical results of Fig. 8 were obtained with $C_v = C_s = 0.95$. The numerically computed pressure profiles are actually

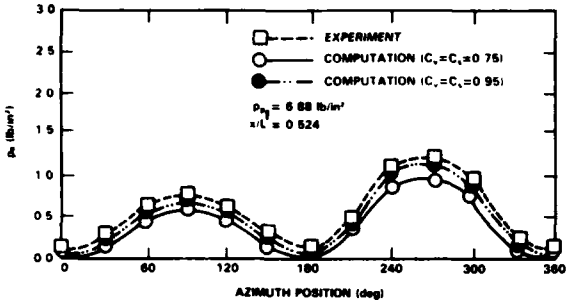


Fig. 7 Quasi-Dynamic Total Pressure vs Cam Position for Two-Per-Rev Cam

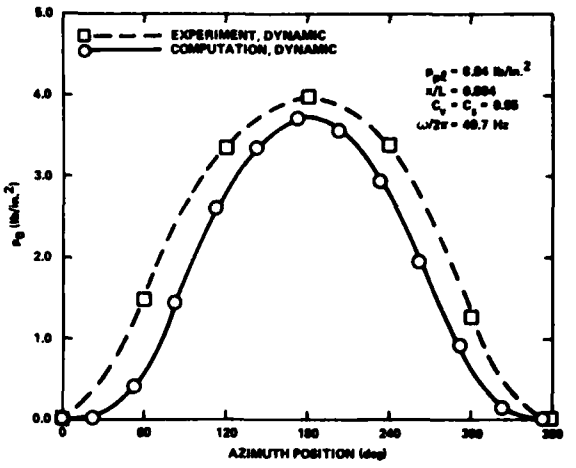


Fig. 8 Dynamic Cyclic Variation of Total Pressure

displaced laterally in azimuth position from the valve area profiles of Fig. 3 due to an approximately 35 deg computed phase shift. This phase shift is principally due to the "capacitance lag" effect caused by the finite pipe volume. A smaller portion of the delay is due to the finite speed of wave propogation, so-called "sonic lag." The phase difference between the valve area setting and the pressure response to it has been eliminated from Fig. 8 for purposes of comparison with the experimental data. Although present in the experiment, phase shift was not an objective of the experimental measurements and is not available from the data. In Figs. 9 and 10 the quasi-dynamic results of Fig. 6 are superimposed onto the dynamic results to demonstrate the effect of unsteady flow on the magnitude and shape of the experimental and numerical pressure responses, respectively. The unsteady effect seems to cause a slight decrease in the peak pressure from the quasi-dynamic results in both the numerical and experimental data. However, this decrease is fairly small; hence, except for the phase difference, the quasi-dynamic results approximate the unsteady results reasonably well.

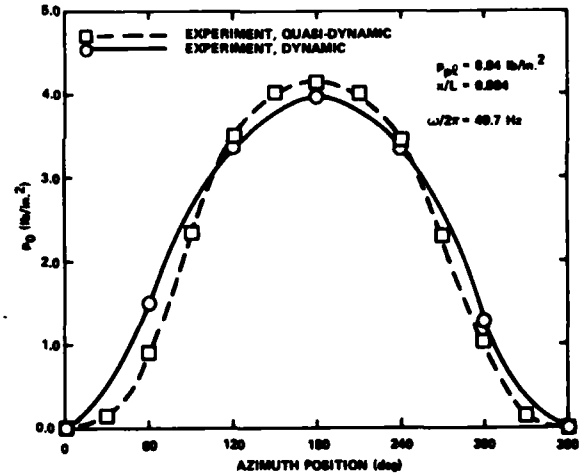


Fig. 9 Comparison of Experimental Dynamic and Quasi-Dynamic Pressure Profiles

## Conclusions

The results presented herein tend to indicate that quasi-one-dimensional flow theory can be applied to predict with reasonable accuracy the pneumodynamics of a circulation control rotor. The implicit finite difference technique used represents an improvement over an explicit method used in a previous computer model but is still restricted to small timesteps. The results further indicate that simple cam-type valving can be used to modulate the flow and pressure of Coanda blowing air to approximately track the variation in the valve opening area. Quasi-dynamic numerical and experimental results can predict dynamic results to a good approximation, but do not reflect the effects of capacitance and sonic lag.

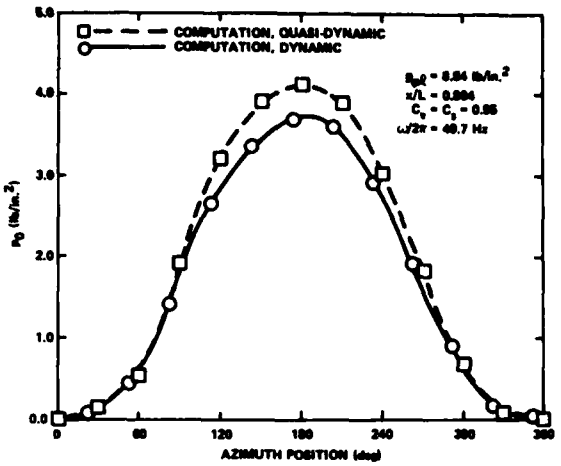


Fig. 10 Comparison of Numerical Dynamic and Quasi-Dynamic Pressure Profiles

## References


1. Reader, K.R., Kirkpatrick, D.G., and Williams, R.M., "Status Report on Advanced Development Programs Utilizing Circulation Control Rotor Technology," Paper No. 44, presented at Associazione Italiana di Aeronautica ed Astronautica Fourth European Rotorcraft and Powered Lift Aircraft Forum, 13-15 Sep 1978, Stresa, Italy.

2. Cheeseman, I.C., and Seed, A.R., "The Application of Circulation Control by Blowing to Helicopter Rotors," Journal of the Royal Aeronautical Society, Vol. 71, No. 451, Jul 1967.

3. Reader, K.R., "Evaluation of a Pneumatic Valving System for Application to a Circulation Control Rotor," NSRDC Report 4070, Naval ship Research and Development Center, May 1973.

4. Conners, F., and Potthast, A.J., "X-Wing Blade Internal Steady and Dynamic Penumatic Properties - Analysis and Preliminary Test Data," Lockheed SP-4875, Lockheed California Company, Nov 1978.

5. Briley, R., and McDonald, P., "Solution of the Three-Dimensional Navier-Stokes Equations by an Implicit Tecynique," Proceedings of the Fourth International Conference on Fluid Dynamics, Lecture Notes in Physics, Vol. 35, Springer-Verlag Berlin, 1975, pp. 105-110.

6. Beam, R.M., and Warming, R.E., "An Implicit Factored Scheme for the Compressible Navier-Stokes Equations," AIAA Journal Vol. 16, No. 4, May 1978, pp. 393-402.

7. MacCormack, R.W., "A Numerical Method for Solving the Equations of Compressible Viscous Flow," AIAA Paper No. 81-0110, AIAA 19th Aerospace Sciences Meeting, 12-15 Jan 1981.

8. White, M.E., and Anderson, J.D., "Application of MacCormack's Implicit Method to Quasi-One-Dimensional Nozzle Flows, AIAA Paper No. 82-0992, AIAA/ASME 3rd Joint Thermophysics, Fluids, Plasma and Heat Transfer Conference, 7-11 Jun 1982, St. Louis, Missouri.

## INITIAL DISTRIBUTION

| Copies | |
|---|---|
| 1 | AASC/Library |
| 2 | HQ USARTL (AVRADCOM)<br>1 DAVDL-D (R.M. Carlson)<br>1 DAVDL-AS (A.W. Kerr) |
| 3 | ATL, USARTL (AVRADCOM)<br>1 Tech Library<br>1 C.E. Hammond/ATA<br>1 W.T. Yeager/Structures |
| 4 | AML, USARTL (AVRADCOM)<br>1 Tech Dir/I.C. Statler<br>1 D.L. Key<br>1 H.A. Morse<br>1 F.H. Schmitz |
| 1 | CMC/Science Advisor<br>A.L. Slafkosky |
| 1 | MCDEC/Tech Advisor |
| 3 | DARPA<br>1 Library<br>1 J.N. Allburn<br>1 R.M. Williams |
| 1 | ONR<br>R.E. Whitehead (Code 432) |
| 1 | NRL/Tech Library (Code 2620) |
| 1 | NAVPSCOL/J. Miller |
| 4 | NAVAIRDEVCEN<br>1 Tech Library<br>1 Tech Director<br>1 R. McGiboney<br>1 G. Woods |
| 1 | USNA/Tech Library |
| 5 | NAVAIRTESTCEN<br>1 Director, TPS<br>1 N. Jubeck<br>1 R. Miller<br>1 R. Richards<br>1 R. Wernecke |

| Copies | |
|---|---|
| 10 | NAVAIRSYSCOM<br>1 Tech Library<br>1 AIR-03A (E.D. Cooper)<br>1 AIR-03B (H. Andrews)<br>1 AIR-310 (T.S. Momiyama)<br>1 AIR-5284 (F.J. O'Brimski)<br>1 AIR-530A (A.R. Somoroff)<br>1 AIR-5301 (R.J. Tracy)<br>1 AIR-5302 (M.J. Dubberly)<br>1 PMA 261<br>1 PMA 2614 (H.F. Burden) |
| 1 | NWC/Tech Library |
| 12 | DTIC |
| 2 | ASD/W-P AFB<br>1 FDL/FIMS, Flight Vehicle Br<br>1 XRH, Design Analysis |
| 1 | AFOSR/Mechanics Div |
| 2 | NASA HQ/RJL<br>1 J. Ward<br>1 D. Maiden |
| 8 | NASA Ames Res Center<br>1 S.B. Anderson (210-10)<br>1 W.H. Deckert (237-2)<br>1 L.A. Haslim (237-3)<br>1 R.M. Hicks (227-8)<br>1 W.R. Johnson (247-1)<br>1 W.J. Snyder<br>1 R.N. Stroub (247-1)<br>1 J. Zuk (237-11) |
| 3 | NASA Langley Res Center<br>1 Tech Library<br>1 R.J. Huston<br>1 W. Young |
| 1 | Rensselaer Polytech Inst<br>R.G. Loewy |

| Copies | |
|---|---|
| 2 | University of Maryland<br>1 A. Gessow<br>1 I. Chopra |
| 1 | University of Tennessee<br>Space Inst/M. Wright |
| 1 | U of West VA/Aero Engr Lib |
| 1 | VA Polytechnic Institute<br>Engr and Mech Library |
| 1 | Analytical Methods, Inc.<br>F.A. Dvorak |
| 1 | ARO/Engr Sciences Div<br>S. Kumar, Asso Dir |
| 1 | Bell Helicopter Textron |
| 2 | Boeing Vertol Co.<br>1 Tech Library<br>1 D.A. Richardson |
| 4 | Hughes Helicopters, Inc.<br>1 Tech Library<br>1 D.C. Borgman<br>1 R. Head<br>1 A.H. Logan |
| 3 | Kaman Aerospace Corp.<br>1 Tech Library<br>1 D.R. Barnes<br>1 A.Z. Lemnios |
| 2 | Lockheed California Co.<br>1 Tech Library<br>1 W.D. Anderson |

| Copies | |
|---|---|
| 1 | Paragon Pacific, Inc.<br>J.H. Hoffman |
| 1 | Piasecki Aircraft Co. |
| 5 | Sikorsky Aircraft<br>1 Library<br>1 R. Blackwell<br>1 E.A. Fradenburgh<br>1 L. Kingston<br>1 D. Smith |
| 1 | Systems Res Labs/R.P. White |
| 3 | United Tech Res Ctr/E. Hartford<br>1 Tech Library<br>1 A.J. Landgrebe<br>1 A. Mensing |

CENTER DISTRIBUTION

| Copies | Code | Name |
|---|---|---|
| 1 | 012 | Director of Technology |
| 1 | 012.3 | Research Coordinator |
| 3 | 1606 | Aerodynamics Collection |
| 10 | 5211.1 | Reports Distribution |
| 1 | 522.1 | TIC (C) +1m |
| 1 | 522.2 | TIC (A) |
| 1 | 9300 | Patent Counsel |